Article published online: 2021-07-26

Comparison of MDCT, MRI and MRI with diffusion-weighted imaging in evaluation of focal renal lesions: The defender, challenger, and winner!

Ankur Goyal, Raju Sharma, Ashu S Bhalla, Shivanand Gamanagatti, Amlesh Seth[1]

Departments of Radiodiagnosis, [1]Urology, All India Institute of Medical Sciences (A.I.I.M.S.), New Delhi, India

Correspondence: Prof. Raju Sharma, Department of Radiodiagnosis, All India Institute of Medical Sciences (A.I.I.M.S.), Ansari Nagar, New Delhi, India. E-mail: raju152@yahoo.com

Abstract

Purpose: To compare the diagnostic performance of multidetector computed tomography (MDCT), magnetic resonance imaging (MRI), and MRI with diffusion-weighted imaging (DWI) in the characterization of focal renal lesions. We also compared MDCT and MRI in the staging of renal cell carcinoma (RCC). **Materials and Methods:** One hundred and twenty adult patients underwent MDCT (40-row and 128-row scanners), MRI (at 1.5 T), and DWI (at b-values of 0 and 500 s/mm^2) for characterization of 225 renal lesions. There were 65 malignant neoplasms (44 RCCs), 25 benign neoplasms, 25 abscesses, 45 pseudotumors, 15 hemorrhagic cysts, and 50 benign cysts. A composite gold standard including histology, typical imaging criteria, and follow-up imaging was employed. To determine the diagnostic performance of imaging modalities, area-under-curve (AUC) was calculated by receiver-operating-characteristic analysis and compared. Fisher's exact test was used to compare the diagnostic accuracies and confidence levels with MDCT, MRI, and MRI + DWI. Cross-tabulation was used to assess the precision of MDCT and MRI in RCC staging. **Results:** AUC for MDCT (0.834) and MRI (0.841) in the classification of benign and malignant lesions were within corresponding 95% confidence interval (CI) (P = 0.88) whereas MRI + DWI had significantly better performance (AUC 0.968, P = 0.0002 and 0.0004, respectively). Both CT and MRI had low specificity (66.9% and 68.8%, respectively), which increased substantially with DWI (93.8%) owing to correct diagnosis of pseudotumors. MRI was superior to CT in diagnosing necrotic RCC and hemorrhagic cysts. MRI + DWI had the highest accuracy (94.2%) in assigning the definitive diagnosis and 97.6% lesions were diagnosed with very high confidence, significantly better than CT and MRI. Both CT and MRI had the same accuracy (86.1%) in RCC staging and evaluation of intravascular thrombi. **Conclusions:** Characterization of renal lesions was most accurate with MRI + DWI. The latter is also the most suitable modality in diagnosing pseudotumors and evaluating patients with renal dysfunction. CT and MRI were equivalent in RCC staging.

Key words: Contrast media; diffusion-weighted MRI; focal renal lesion; MRI; multidetector CT; renal cell carcinoma

Introduction

Renal lesions are frequently detected incidentally and at an early stage with the widespread use of various imaging modalities. Incidence of renal cell carcinoma (RCC), the most common renal malignancy, is also rising.[1] Tumor stage is the

Access this article online	
Quick Response Code:	Website: www.ijri.org
	DOI: 10.4103/ijri.IJRI_40_17

Cite this article as: Goyal A, Sharma R, Bhalla AS, Gamanagatti S, Seth A. Comparison of MDCT, MRI and MRI with diffusion-weighted imaging in evaluation of focal renal lesions: The defender, challenger, and winner!. Indian J Radiol Imaging 2018;28:27-36.

most important prognostic factor in RCC affecting patient survival and management.[2] Sonography is a screening modality to detect renal lesions, which is followed by computed tomography (CT) and/or magnetic resonance imaging (MRI) for further evaluation. Multidetector CT (MDCT) is the preferred investigation because of wide availability, low cost, shorter acquisition time, and excellent spatial resolution. MRI offers a radiation-free alternative with better soft-tissue contrast and superior demonstration of contrast enhancement.[3] There is paucity of literature comparing MDCT and MRI in the characterization and extent delineation of renal lesions. Moreover, the few published studies[2,4-7] employed old scanners, implying that their results are not reliable in the present era. With the availability of state-of-the-art techniques, it is debatable which imaging modality is best suited for evaluation of renal lesions.[7]

In the absence of macroscopic fat, identification of enhancing soft tissue in a renal lesion at contrast-enhanced imaging has been the accepted criterion for malignancy. However benign solid masses, inflammatory lesions, complex benign cysts, and pseudolesions in normal and diseased kidneys can mimic the imaging appearance of RCC. Hence, despite a thorough radiological evaluation, the incidence of benign pathologies at surgery for presumed renal malignancy remains significant.[8] Contrast-enhanced CT (CECT) is associated with radiation exposure and risk of contrast-induced-nephropathy whereas MR contrast agents predispose to nephrogenic systemic fibrosis in patients with renal insufficiency. Hence, imaging modalities without employing contrast administration are ideal.

Diffusion-weighted imaging (DWI) is one such diagnostic proposition, which provides useful information with minimum time penalty.[9] Another emerging technique is contrast-enhanced ultrasound, which may prove useful in the evaluation of complex cystic lesions and in patients with renal dysfunction. Previous researchers have investigated the role of diffusion-weighted MRI (DW-MRI) in characterization of focal renal masses,[10-19] parenchymal renal disease[12,19-23] and renal infections.[18,24,25] Of these, only one study[14] compared the accuracy of DWI with contrast-enhanced MRI in evaluation of focal renal lesions. There are no consolidated data on the utility of DWI in renal lesion evaluation, over and above the existing imaging modalities.

The purpose of this study was to compare the diagnostic performance of current-generation MDCT, MRI, and MRI with DWI in the characterization of focal renal lesions. In addition, we also compared MDCT and MRI in the staging of RCCs.

Materials and Methods

Study population and data collection

A cross-sectional study to evaluate focal renal lesions using MDCT and MRI along with DWI was undertaken at our institute. Patient recruitment was done prospectively from November, 2008 to November, 2012 . The study was approved by the Institutional Ethics Committee, and informed consent was taken from all the patients. Adult patients (≥18 years) with sonographically-detected renal lesions requiring further imaging work-up were included. Exclusion criteria were pregnancy, contraindications to MRI examination, and patients in whom sonography alone was diagnostic (simple benign cysts). Simple renal cysts were also detected incidentally in patients undergoing imaging for other renal lesions and these were included in the analysis. One hundred and thirty patients were recruited in the study, of which 10 were excluded because they were lost to follow-up. The final study cohort consisted of 120 patients who underwent MDCT, MRI, and DW-MRI for characterization of renal lesions (78 men, 42 women; mean age 42.7 years, age range 18–85 years). The interval between MDCT, MRI, and DW-MRI examinations was less than 2 weeks.

In patients with multiple similar lesions, maximum of three largest lesions per kidney were selected for analysis. This resulted in a total of 225 renal lesions that comprised 65 malignant neoplasms [44 RCCs in 40 patients, 10 transitional cell carcinomas (TCCs) in 10 patients, 11 miscellaneous lesions in 5 patients] and 25 benign neoplasms [20 angiomyolipomas (AMLs) in 12 patients, 4 oncocytomas in 4 patients, 1 leiomyoma]. In addition, there were 25 abscesses in 20 patients, 45 pseudotumors (40 in diseased and 5 in normal kidneys) in 25 patients and 10 hemorrhagic cysts in 3 patients. Five hemorrhagic cysts and 50 benign cysts (Bosniak category I, II, and IIF) were found incidentally in patients undergoing evaluation of other renal lesions. Bosniak category I cysts <10 mm in size were not included in analysis.

A composite gold standard including histology, typical imaging criteria, and follow-up imaging was employed. All malignant lesions (65/65) were proven pathologically (among RCCs, 36 were excised and 8 were biopsied under sonographic guidance, 9/10 TCCs were operated whereas one underwent biopsy, all the patients with miscellaneous malignant lesions underwent sonography guided tissue-sampling). Six AMLs were operated (2 underwent resection because of large size whereas the other 4 had no evidence of fat on any imaging modality, thus deemed malignant) whereas rest 14 were diagnosed on the basis of typical imaging findings. All the miscellaneous benign neoplasms were operated because these were labelled malignant on all imaging modalities. In abscesses, 15 patients underwent ultrasound-guided aspiration and 5 showed complete resolution on imaging follow-up (mean follow-up 2.4 months, range 1–6 months). In case of pseudotumors, 16 patients underwent ultrasound-guided biopsy of the renal lesions, which did not show any evidence of malignancy whereas 9 patients demonstrated sonographic

stability of the lesions for at least 15 months (documented by 3-monthly follow-up sonographic evaluation, mean follow-up of 20 months, range 15–36 months). Absence of contrast enhancement, presence of T1 hyperintense fluid component, and sonographic stability on follow-up imaging was taken confirmatory for hemorrhagic cysts. One patient was operated because of suspicion of underlying malignancy on imaging; however, histopathology revealed no evidence of malignancy in the hemorrhagic cyst. In case of benign cysts, imaging findings were considered sufficient as reference criterion. Surgery and/or histopathologic examination were performed within 3 weeks after imaging. Surgico-pathological gold standard for staging was available in 36 RCCs.

Multidetector computed tomography

All studies were performed on 40-row (Somatom Sensation 40, Siemens, Erlangen, Germany) and 128-row (Somatom Definition AS+, Siemens, Erlangen, Germany) MDCT scanners. Scans were obtained with a detector collimation of 24 × 1.2 mm (on 40-row) or 128 × 0.6 mm (on 128-row) at 120 kV and 70–90 effective mAs. A multiphasic imaging protocol comprising unenhanced, corticomedullary, nephrographic, and delayed phase was employed. One hundred milliliter of nonionic iodinated contrast media (iodine 300 mg/mL) was injected through an intravenous cannula using a pressure injector (at rate of 4 mL/s). In case there was no suspicion of neoplastic renal lesion, unenhanced phase was followed by single contrast-enhanced acquisition at 60–70 s from the start of injection. Contrast medium was withheld if the serum creatinine value was >1.5 mg/dL. Coronal and sagittal multiplanar reconstructions (MPRs), maximal intensity projections (MIPs), and volume rendering techniques (VRT) were frequently used, as and when required.

Magnetic resonance imaging

MR imaging was done at 1.5 Tesla (Siemens, Avanto, Erlangen, Germany) (maximum gradient strength 45 mTm^{-1}, maximum slew rate 200 $mTm^{-1}s^{-1}$) in supine position using a phased-array body coil. Two anteriorly placed 6-element body matrix coils and two posterior spine clusters (three channels each) were employed. The imaging protocol is shown in Table 1. Dynamic contrast-enhanced MR was performed using Gadobenate dimeglumine (MultiHance, Bracco, Milan, Italy), injected via a dual head pressure injector (Spectris Solaris, Medrad, Philadelphia, Pennsylvania, USA) at a rate of 2 mL/s followed by 20 mL saline flush at the same rate. The dose employed was 0.1 mmol/kg body weight, and contrast medium was withheld if the estimated GFR was less than 30 mL/min/1.73m^2. Post-contrast acquisition was done in the axial plane in arterial, cortico-medullary, nephrographic, and pyelographic phases and in coronal plane in nephrographic phase. A pre-contrast axial acquisition using the same parameters was also done so that the subtracted images could be generated.

Diffusion-weighted magnetic resonance imaging

Respiratory triggered FS (spectral fat suppression) spin echo–echo planar imaging (SE-EPI) axial diffusion-weighted sequence at b values of 0 and 500 s/mm^2 was done before contrast administration, using generalized autocalibrating partially parallel acquisition (GRAPPA) with twofold acceleration factor and diffusion gradients applied in all three orthogonal directions separately. The DW sequence was respiratory triggered using navigator-triggered prospective acquisition correction technique (PACE) in which diaphragmatic position is assessed periodically by navigator echoes. The parameters used are shown in Table 1, and acquisition time was 2–4 min (depending on patient's respiratory cycle). Trace DWI and apparent diffusion coefficient (ADC) maps were derived automatically on a voxel-by-voxel basis.

Image analysis

Two experienced radiologists (having 20 and 15 years of experience in abdominal imaging) interpreted all the imaging data together in consensus; they were blinded to

Table 1: Parameter summary of conventional and DW-MRI sequences

MR sequence		TR/TE (ms)	Flip angle (degrees)	Slice thickness (mm)	Distance factor (%)	No. of averages	Receiver bandwidth (Hz/pixel)	Field of view	Matrix
True FISP 2D axial	bh	3.4/1.4	39	5	30	1	490	263×350	288×512
True FISP 2D coronal	bh	3.4/1.4	36	5	10	1	490	380×380	410×512
T1W 2D FLASH axial dual echo									
In phase	mbh	125/4.76	70	5	30	1	500	278×370	288×512
Out of phase		125/2.34							
T1 FS FLASH 2D	mbh	203/4.8	70	5	10	1	180	263×350	288×512
T2W FS TSE axial	mbh	2520/100	137	5	30	1	260	278×370	288×512
T2W FS TSE coronal	mbh	2700/100	137	5	10	1	260	410×430	171×256
FS axial DW-MRI at b=0, 500 s/mm^2	RT	1600/62	90	7	30	6	1735	249×380	94×192
Post contrast T1W FS 3D VIBE axial	bh	5.1/2.3	10	3	20	1	300	253×450	158×512
Post contrast T1W FS 3D VIBE coronal	bh	5.0/2.3	10	3	20	1	300	400×400	322×512

TrueFISP: True fast imaging and steady precession, FLASH: Fast low angle shot, FS: Fat suppressed, TSE: Turbo spin echo, bh: Breath hold, mbh: Multi breath hold, RT: Respiratory triggered, VIBE: Volume interpolated breath hold examination, TR: Repetition time, TE: Echo time

the final diagnosis. While analyzing the findings of one modality, the interpreting radiologists were blinded to other modalities. Characterization of the renal lesions into benign/malignant/indeterminate was done on CT, MRI, and MRI with DWI. A definitive/most likely diagnosis was given on all three modalities, and a confidence score was assigned to that diagnosis using three-point ordinal scale (1- average confidence, 2- high confidence, and 3- very high confidence). For miscellaneous renal malignancies, imaging diagnosis of RCC or malignant renal lesion was considered consistent with the reference standard. On DWI, presence of restricted diffusion in the solid enhancing components of a renal lesion affirmed malignancy. Absence of diffusion restriction in solid lesion ruled out malignancy. Presence of marked restriction of diffusion in the fluid component favoured abscesses. Free diffusion in cystic lesions clinched the diagnosis of benign cysts.

Pathologically confirmed malignant lesions were termed true-positive and correctly diagnosed benign lesions as true-negative. If the lesion was benign but deemed malignant on imaging, it was classified as false positive, whereas if histology revealed malignant instead of suspected benign lesion, it was adjudged false-negative. Based on these, validity parameters including sensitivity, specificity, positive and negative predictive values (PPV and NPV), and accuracy were calculated. TNM staging was assigned for RCCs as per the American Joint Committee on Cancer (AJCC) staging system. Wherever applicable, the nature and extent of intravascular thrombus was assessed on all modalities.

Statistical analysis

SPSS software (version 17.0, SPSS, Chicago, Illinois, USA) was used. Receiver operating characteristic (ROC) analysis was done to determine the diagnostic performance of MDCT, MRI, and MRI + DWI in the differentiation of benign and malignant lesions. Area under the curve (AUC) was calculated by logistic regression analysis and corresponding 95% confidence interval (CI) obtained. Differences between ROC curves and AUC values were assessed on the basis of 95% CI. Fisher's exact test was used to compare the diagnostic accuracies and confidence levels of MDCT, MRI, and MRI + DWI in the characterization of renal lesions. Cross-tabulation was used to assess the accuracy of MDCT and MRI in staging of RCCs. Two-tailed *P* values were calculated and $P < 0.05$ was taken as statistically significant.

Results

MDCT, MRI, and DWI could identify all the 225 renal lesions and good quality images were obtained in all the patients. The mean lesion size (on T2-weighted MR images) was 4.7 ± 3.1 cm (range, 1.5–20 cm). CT and MR contrast could not be administered in any of the 20 patients of pseudotumors in diseased kidneys, 5 patients of abscesses, and 1 patient of RCC owing to deranged renal functions.

Comparison of multidetector computed tomography, magnetic resonance imaging, and magnetic resonance imaging + diffusion-weighted imaging for classification of renal lesions into benign or malignant

Out of the 225 renal lesions evaluated, there were 160 benign and 65 malignant lesions based on the reference standard. Lesions characterized as indeterminate on imaging were excluded from further analysis. Results are shown in Table 2 and Figure 1. Seven lesions remained indeterminate on CT of which 3 were benign and 4 turned out to be malignant. On MRI and MRI + DWI, only 3 lesions remained indeterminate, which were malignant on reference standard (1 RCC, 2 squamous cell carcinomas). AUC for MDCT and MRI were comparable ($P = 0.88$) and within corresponding 95% CI [Figure 1]. AUC of MRI + DWI was significantly higher than that of both MDCT and MRI ($P = 0.0002$ and 0.0004, respectively) and outside the corresponding 95% CI [Figure 1].

Comparison of multidetector computed tomography, magnetic resonance imaging, and magnetic resonance with diffusion-weighted imaging in assigning definitive diagnosis

While MRI fared marginally better than MDCT (accuracy 77.8% vs 72.9%, $P = 0.27$), MRI + DWI had the highest accuracy (94.2%) in assigning definitive diagnosis ($P < 0.0001$ vs both CT and MRI) [Table 3]. Figure 2 shows one such lesion which could not be diagnosed on CT or MRI but correctly interpreted on MRI + DWI.

Assessment of degree of confidence in cases correctly diagnosed on imaging

In lesions correctly diagnosed on the basis of respective imaging modality, the distribution, as per the confidence

Table 2: Validity parameters and ROC analysis for MDCT, MRI and MRI + DWI in classification of renal lesions as benign/malignant (total 225 lesions)

	MDCT	MRI	MRI + DWI
True positive TP	61	62	62
False positive FP	52	50	10
True negative TN	105	110	150
False negative FN	0	0	0
Indeterminate on imaging	7	3	3
Sensitivity %	**100**	**100**	**100**
Specificity %	**66.9**	**68.8**	**93.8**
Positive predictive value PPV	54	55.4	86.1
Negative predictive value NPV	100	100	100
Accuracy %	**76.1**	**77.5**	**95.5**
Area under curve AUC	**0.834**	**0.841**	**0.968**
Standard error SE	0.026	0.026	0.012
95% confidence intervals			
Lower bound	0.783	0.790	0.945
Upper bound	0.886	0.891	0.991

level of making the diagnosis, is shown in Figure 3. Table 4 depicts the proportion of various renal lesions diagnosed correctly with very high confidence on different modalities. Overall, MRI mildly increased the diagnostic confidence (P = 0.32 for confidence level 3, i.e. very high confidence), and with the addition of DWI, 97.6% lesions were diagnosed with very high confidence ($P < 0.0001$ vs both CT and MRI). Figure 4 demonstrates an example where MR with DWI increased the diagnostic confidence.

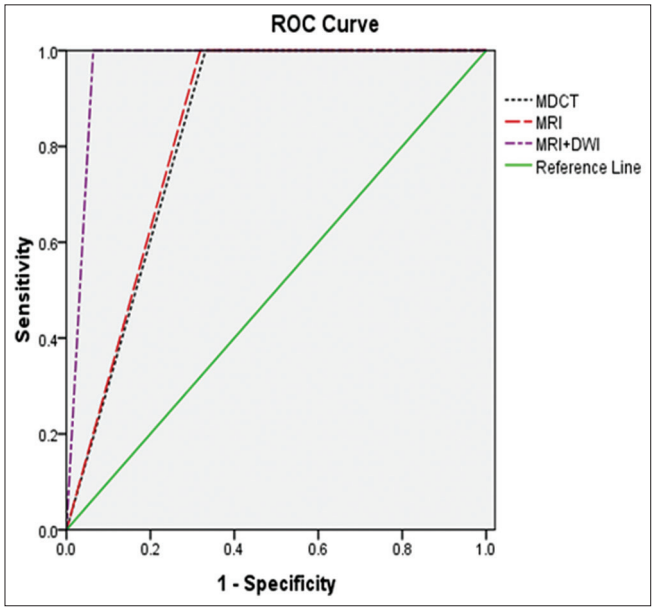

Figure 1: Graphical comparison of ROC curves for MDCT (dotted black line), MRI (dashed red line), and MRI + DWI (dot and dash purple line) in the differentiation of benign and malignant renal lesions. AUC is the largest for MRI + DWI (0.968) and similar for CT (0.834) and MRI (0.841). Straight diagonal green line spanning the middle of the graph indicates an AUC of 0.5

Comparison of multidetector computed tomography and magnetic resonance imaging in TNM staging of renal cell carcinomas

TNM staging on both CT and MRI was compared with the surgico-pathological reference standard in 36 RCCs. Both

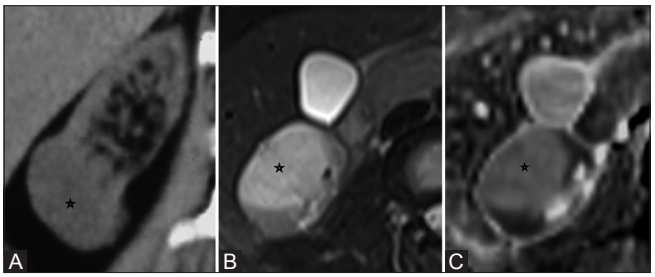

Figure 2 (A-C): Pseudotumour in diseased kidney in a 45-year-old female patient, not diagnosed on CT or MR but correctly interpreted on DWI. (A) Coronal unenhanced CT image shows ill-defined, mildly hypodense, exophytic mass lesion (asterisk) in the lower pole of the right kidney. Contrast could not be administered because of renal dysfunction. (B) Axial T2-weighted MR image shows that the lesion is hyperintense (asterisk). Solid "ball-type" morphology and hyperintensity on T2-weighted image raised the suspicion of malignant mass on CT and MRI. (C) Axial ADC map (generated from DWI) demonstrates the lesion to be hyperintense (asterisk) suggesting no diffusion restriction within the lesion. Absence of diffusion restriction within a solid mass lesion ruled out malignancy. Ultrasound-guided biopsy did not reveal any evidence of malignancy

Table 3: Number of lesions correctly diagnosed on various modalities

Final diagnosis	Number of lesions on reference standard	Lesions correctly diagnosed by MDCT	Lesions correctly diagnosed by MRI	Lesions correctly diagnosed by MRI + DWI
Renal cell carcinoma	44	42	43	43
Transitional cell carcinoma	10	10	10	10
Miscellaneous				
Squamous cell carcinoma	2	0	0	0
Primitive neuroectodermal tumor	1	1	1	1
Lymphoma	2	2	2	2
Metastases	6	6	6	6
Total malignant renal lesions	**65**	**61**	**62**	**62**
Typical angiomyolipoma (AML)	16	16	16	16
Lipopenic AML	4	0	0	0
Oncocytoma	4	0	0	0
Leiomyoma	1	0	0	0
Total benign neoplasms	**25**	**16**	**16**	**16**
Abscesses	**25**	**25**	**25**	**25**
Pseudotumors in chronic kidney disease	40	0	3	40
Pseudotumors in normal kidneys (normal variants like dromedary hump)	5	4	5	5
Total renal pseudotumors	**45**	**4**	**8**	**45**
Hemorrhagic cysts	**15**	**8**	**14**	**14**
Benign cystic lesions	50	50	50	50
TOTAL (percentage of lesions correctly diagnosed)	**225**	**164 (72.9%)**	**175 (77.8%)**	**212 (94.2%)**

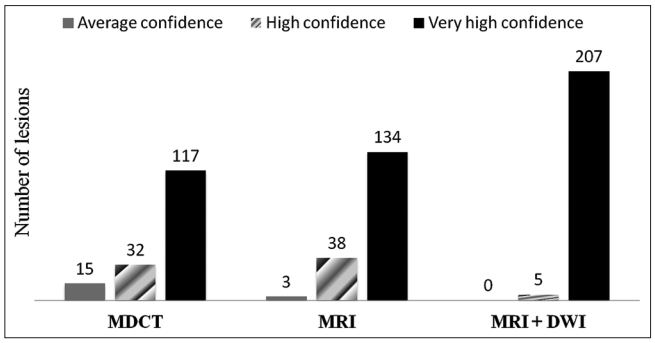

Figure 3: Distribution of the degree of diagnostic confidence on various imaging modalities. MRI + DWI diagnosed 97.6% of the renal lesions with very high confidence

Table 4: Valid percentage of various lesions diagnosed correctly with very high confidence on imaging modalities

	Valid percentage for MDCT	Valid percentage for MRI	Valid percentage for MR with DWI
Malignant renal lesions	70	75.4	96.7
Benign neoplasms	87.5	100	100
Abscesses	16	32	100
Pseudotumors	100	62.5	100
Hemorrhagic cysts	50	71.4	85.7
Benign cysts	98	98	100
All renal lesions	71.5	76.6	97.6

modalities were similar in assigning TNM stage [Table 5]. For overall stage, both had an accuracy of 86.1% (31/36 tumors), and the least accuracy was for stage III (76.9%) [Table 5]. Overall, 3 RCCs were overstaged and 2 were understaged on imaging. Regarding T-stage, both had an accuracy of 88.9% (32/36 tumors) [Table 6]. Perirenal fat invasion was missed in 3 RCCs and wrongly detected in one. Regarding nodal staging, both modalities correctly diagnosed absence of lymphadenopathy (N0) in 29 RCCs, N1 in 4 patients, and N2 in 1 patient (accuracy 34/36, 94.4%). Two patients were found to have reactive lymphadenopathy, whereas imaging assigned N2 stage. M-staging was not compared because of lack of gold standard for metastatic work-up.

Six patients were found to have malignant intravascular thrombus on surgico-pathological reference standard. Nature of the thrombus was correctly predicted by MDCT, MRI, and MR with DWI in all these patients [Figure 5]. The cranial most extent of the malignant thrombus could be accurately demonstrated by MDCT and MRI in all these patients (1 patient had involvement of only renal vein, 4 had involvement of retrohepatic IVC, and 1 had thrombus extending above the level of diaphragm into the right atrium) [Figure 5].

Discussion

At present, multiphasic contrast-enhanced MDCT is the workhorse in renal lesion evaluation whereas MRI is a

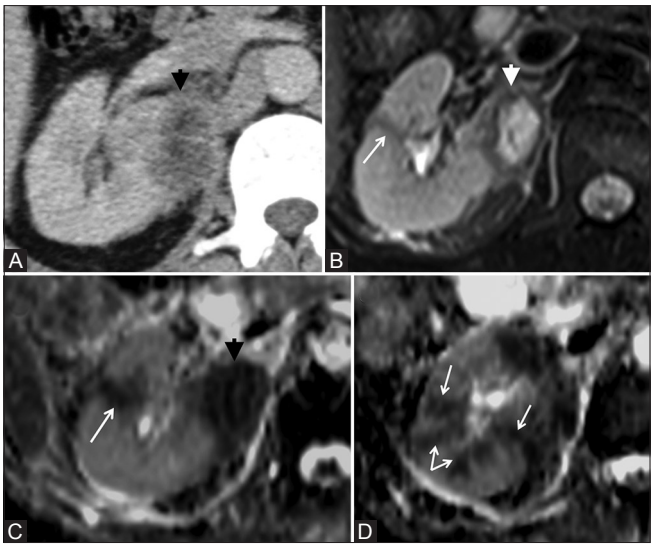

Figure 4 (A-D): A 49-year-old male patient presented with right flank pain, fever, and polymorphonuclear leukocytosis. (A) Axial contrast-enhanced CT image shows an ill-defined heterogeneously enhancing mass lesion (arrowhead) in the medial cortex of interpolar region of the right kidney with infiltration into perirenal space. Considering the clinical details, diagnosis of abscess was made but confidence level of making this diagnosis was just average. (B) Axial T2-weighted MR image adds to the diagnostic confidence by demonstrating central hyperintense region surrounded by thick hypointense rim (arrowhead). Note is also made of a hypointense band in the lateral cortex of the kidney (arrow) and perirenal fascial thickening. (C) Axial ADC map demonstrates very dark signal in the lesion (arrowhead) indicative of marked restriction of diffusion, especially in the T2 hyperintense fluid component, thus making the diagnosis of renal abscess almost certain. The hypointense band seen previously on T2-weighted MR image also shows restricted diffusion. (D) Axial ADC map (at cranial level) shows multiple bands (some of them are wedge-shaped) of restricted diffusion (arrowheads) in the renal parenchyma suggesting acute pyelonephritis, further favouring the inflammatory etiology. Follow-up MR imaging (not shown) after 6 weeks of intravenous antibiotics showed near-complete resolution of the abscess

problem-solving adjunct modality.[26] Only a few studies have compared MDCT and MRI in characterization of renal lesions[4,7] and in staging of RCC,[2,4-7] with the most recent study employing 16-slice CT in only 28 patients. DWI is yet to find its place in the renal imaging protocol because there are no studies highlighting its comparison with CT or MR. Because of the presence of renal dysfunction, CT/MR contrast could not be administered in 26 patients (21.7%) in our study. This observation endorses the need for a non-contrast imaging modality for renal lesion evaluation in such patients.

Differentiation of benign and malignant renal lesions is valuable in deciding the optimal management and prognostication. All three modalities had 100% sensitivity in the diagnosis of malignant lesions, and hence no malignant lesion was misclassified as benign. Both CT and MRI had relatively low specificity because of misdiagnoses of non fat-containing benign neoplasms and pseudotumors. Specificity increased substantially with the addition of DWI owing to correct diagnosis of all the pseudotumors.

Table 5: Overall Staging results of MDCT and MRI compared with gold standard in RCC (*n*=36)

MDCT MRI	Gold standard				Total (CT/MR)
Stage	I	II	III	IV	
I	15	0	1	0	16
II	0	5	1	0	6
III	0	1	10	0	11
IV	1	0	1	1	3
Total (gold std)	16	6	13	1	36

Table 6: T-Staging results of MDCT and MRI compared with gold standard in RCC (*n*=36)

MDCT MRI	Gold standard							Total (CT/MR)
T-Stage	1a	1b	2	3a	3b	3c	4	
1a	4	0	0	0	0	0	0	4
1b	0	12	0	2	0	0	0	14
2	0	0	5	1	0	0	0	6
3a	0	0	1	5	0	0	0	6
3b	0	0	0	0	5	0	0	5
3c	0	0	0	0	0	1	0	1
4	0	0	0	0	0	0	0	0
Total (gold std)	4	12	6	8	5	1	0	36

Both CT and MRI were found to have similar diagnostic performance in classifying benign and malignant lesions whereas MRI + DWI fared significantly better.

All the 16 fat-containing typical AMLs were correctly diagnosed on all modalities. However, none of the remaining 9 benign neoplasms could be diagnosed preoperatively and were falsely termed malignant on all modalities. Walter *et al*.[4] observed that distinction between solid benign and malignant lesions was not possible with CT or MR imaging. Similar high sensitivity and low specificity for CT and MRI were reported by Beer *et al*.[7] who attributed this to the misdiagnosed oncocytomas in their study. This reflects a common imaging problem that, except for typical AMLs, no robust imaging criteria exist for differentiating benign neoplasms from RCC and they end up getting surgically resected.[7,27-30] Recent studies have suggested new criteria for diagnosing benign neoplasms on CT, MRI, and DWI; however, these need to be validated prospectively.[14,29,31-34]

In assigning definitive diagnosis, MRI performed slightly better than CT, especially in diagnosing necrotic RCCs (devoid of obvious enhancing soft tissue component), hemorrhagic cysts, and pseudotumors, and the number of indeterminate lesions was also reduced. Addition of DWI to MRI enabled precise diagnosis of all the pseudotumors in diseased kidneys, making it the most accurate modality.

CT correctly diagnosed 61/65 malignant renal lesions. MRI and MRI + DWI could correctly diagnose one additional RCC, which was indeterminate on CT because of lack of

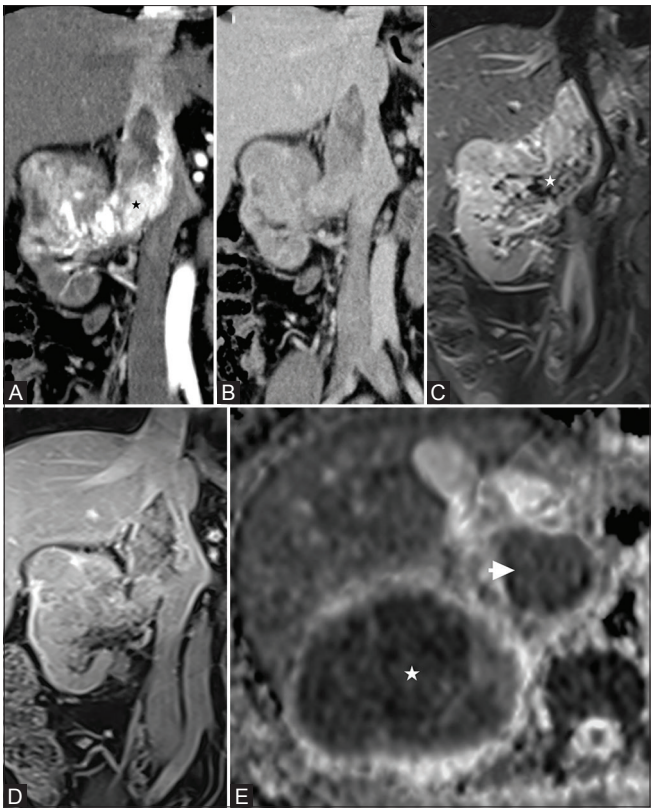

Figure 5 (A-E): Comparison of MDCT, MRI, and DWI in demonstrating malignant intravascular thrombus. (A) Coronal arterial phase CT image shows lobulated mass in the right kidney with contiguous thrombotic extension into right renal vein and inferior vena cava (IVC). The intravascular thrombus is showing arterial enhancement (asterisk), indicative of neovascularity, suggesting malignant thrombus. (B) Coronal venous phase CT image shows heterogeneous enhancement in the primary mass as well as the contiguous thrombus. Note that the thrombus is seen as nonocclusive filling defect in the IVC and is causing expansion of the involved segments. Also note that the entire extent of the thrombus is well seen on different phases of MDCT and clearly depicted in coronal reconstructions. (C) Coronal T2-weighted MR image beautifully demonstrates the mass and the thrombus to be of similar high signal intensity, further favoring malignant thrombus. Corresponding to the areas of neovascularity in the malignant thrombus, flow voids are seen on T2-weighted images (asterisk). (D) Coronal venous phase MRI image shows heterogeneous enhancement in the primary mass as well as the contiguous thrombus and gives similar information as contrast-enhanced CT. (E) Axial ADC map shows dark signal within the renal mass (asterisk) as well as the IVC thrombus (arrowhead), indicating restricted diffusion. The ADC values of primary mass and IVC thrombus were comparable [1.12 and 1.09 ($\times 10^{-3}$ mm^2/s), respectively]. Presence of restricted diffusion with ADC values similar to that of primary mass endorse the diagnosis of malignant thrombus. The malignant thrombus is extending into the retrohepatic IVC below the level of diaphragm and the cranial most extent is same in both CT and MR (A-D)

enhancing soft tissue component. T2-weighted MR images demonstrated nondependent nodular soft tissue component along the walls which showed restricted diffusion on DWI. Compared to CT, MRI correctly diagnosed 6 additional hemorrhagic cysts (Two of these cysts were indeterminate whereas 4 had no evidence of hemorrhage on CT). Walter *et al*.[4] reported equal accuracy of CT and MRI in the characterization of renal lesions; however, their small study

population did not include necrotic RCCs or hemorrhagic cysts.

All the 40 pseudotumors in diseased kidneys were deemed malignant on CT and 37 of these remained misclassified even on MRI; however, absence of diffusion restriction ruled out malignancy in all these lesions [Figure 2]. These pseudotumors represent focal nodular compensatory hypertrophy of relatively preserved renal parenchyma in chronic kidney disease.[19] Solid ball-type morphology and hyperintensity on T2-weighted images were the deceptive factors on CT and MR [Figure 2]. Another reason for their misdiagnosis may be that enhancement characteristics could not be evaluated because renal dysfunction precluded the use of contrast media.

The degree of diagnostic confidence was the lowest with CT, marginally increased with MRI, and greatly improved by the addition of DWI [Figure 3]. This was especially evident in abscesses where 100% of the lesions could be diagnosed with certainty based on markedly restricted diffusion in the fluid components [Figure 4]. Even in malignant lesions, restricted diffusion in the solid components boosted the diagnostic confidence.

Thus, MRI + DWI appears to be the best investigation in the characterization of focal renal lesions. DWI improves the accuracy and diagnostic confidence of conventional MRI (including contrast-enhanced MR) and proves to be an excellent addition to the imaging armamentarium in evaluation of renal lesions. It can be easily incorporated into the currently existing MR protocols without any additional cost, time, or risk of nephrotoxicity. Without contrast administration, diagnostic utility of CT is lost completely and is markedly reduced in case of MRI. DWI offers the best solution to characterize renal lesions in patients with renal dysfunction where contrast administration is not desirable. Nevertheless, owing to wide availability, low cost, and shorter acquisition time, MDCT may continue to be the first-line investigation for evaluation of common renal lesions.

Dramatic improvement in the image quality since its introduction has led to increased accuracy of MDCT in the preoperative staging of RCC.[35] We found no difference between MDCT and MRI either in overall staging (both had accuracy of 86.1%) or in T and N-staging of RCC. Inaccuracies were due to misinterpretation of perirenal fat invasion and false labelling of enlarged reactive lymph nodes as malignant. Previous studies[2,4,7] have reported lower accuracy for both modalities in staging of RCC. This may be ascribed to state-of-the-art MDCT and MRI scanner in our study. It is a well documented fact that spread of tumor into the perinephric fat is difficult to diagnose[2,4] and reactive nodes can be misinterpreted as metastatic based on size criteria.[7]

The nature and extent of the tumor thrombus affects the decision to operate, the surgical approach, and the cranial-most extension of a possible resection.[5] Nature and extent of the intravascular thrombus was correctly diagnosed by both CT and MR in all cases [Figure 5]. On DWI as well, the nature of thrombus was accurately predicted based on the presence of restricted diffusion with ADC values similar to that of primary mass [Figure 5]. We did not have any case of pathologically proven benign thrombus; however, bland thrombi have been reported to have higher ADC values and thus can be differentiated on DWI.[36] Our results are in agreement with the previous studies.[5,6] Thus, the presumed advantages of MRI, such as multiplanar imaging and better delineation of tumor thrombus,[37] no longer apply with the use of multiphasic MDCT, which permits high quality isotropic multiplanar reformatting. Nevertheless, one should keep in mind that detection of malignant thrombus on CT is based on demonstration of arterial enhancement and non-opacification of the involved vein on venous phase. MRI, in addition to similar findings, beautifully depicts the thrombus on T2-weighted images.[5] Thus, MRI does not rely entirely on contrast medium to differentiate thrombus from flowing blood, rather has intrinsic contrast superiority to CT.[5] T2-weighted images and DWI can prove beneficial in evaluation of tumor thrombus in cases where contrast-enhanced imaging is contraindicated.

There are a few limitations of our study. We had a heterogeneous and unusual spectrum of renal lesions with a significant number of pseudotumors. This may be attributed to the fact that the study was conducted in a tertiary care center where problematic/indeterminate renal masses constituted a substantial proportion of referrals. Second, histopathology was not available for all the lesions. Rather we employed a composite gold standard because tissue sampling in case of unequivocal benign cysts or typical AMLs was not justified. Third, imaging analysis was done by consensus and interobserver variability was not evaluated.

Conclusion

In conclusion, we found that both MDCT and MRI have low specificity and benign neoplasms without demonstrable fat continue to pose a diagnostic challenge. MRI was more accurate than CT in diagnosing necrotic RCCs and hemorrhagic cysts. DWI was the only modality to confidently rule out malignancy in pseudotumours, majority of which were misdiagnosed on conventional imaging. MRI + DWI had the highest accuracy not only in distinguishing benign and malignant lesions but also in assigning the definitive diagnosis with confidence, thus proving to be the best modality for characterization. Thus, DWI should always be included in the MR evaluation of renal lesions. Both CT and MRI had similar high accuracy in staging of RCC and intravascular thrombus evaluation. MRI + DWI is the

most suitable modality in evaluating patients with renal dysfunction, not only for characterization of renal lesions but also in evaluating intravenous thrombosis.

Financial support and sponsorship
Nil.

Conflicts of interest
There are no conflicts of interest.

References

1. Pallwein-Prettner L, Flöry D, Rotter CR, Martinez-Moya P, Romero-Calvo I, Suarez MD, *et al*. Assessment and characterisation of common renal masses with CT and MRI. Insights Imaging 2011;2:543-56.
2. Hallscheidt PJ, Bock M, Riedasch G, Zuna I, Schoenberg SO, Soder M, *et al*. Diagnostic accuracy of staging renal cell carcinomas using multidetector-row computed tomography and magnetic resonance imaging: A prospective study with histopathologic correlation. J Comput Assist Tomogr 2004;28:333-9.
3. Prasad SR, Dalrymple NC, Surabhi VR. Cross-sectional imaging evaluation of renal masses. Radiol Clin North Am 2008;46:95-111.
4. Walter C, Kruessell M, Gindele A, Brochhagen HG, Gossmann A, Landwehr P. Imaging of renal lesions: Evaluation of fast MRI and helical CT. Br J Radiol 2003;76:696-703.
5. Hallscheidt PJ, Fink C, Haferkamp A, Bock M, Luburic A, Zuna I, *et al*. Preoperative staging of renal cell carcinoma with inferior vena cava thrombus using multidetector CT and MRI: Prospective study with histopathological correlation. J Comput Assist Tomogr 2005;29:64-8.
6. Lawrentschuk N, Gani J, Riordan R, Esler S, Bolton DM. Multidetector computed tomography vs magnetic resonance imaging for defining the upper limit of tumour thrombus in renal cell carcinoma: A study and review. BJU Int 2005;96:291-5.
7. Beer AJ, Dobritz M, Zantl N, Weirich G, Stollfuss J, Rummeny EJ. Comparison of 16-MDCT and MRI for characterization of kidney lesions. AJR Am J Roentgenol 2006;186:1639-50.
8. Kutikov A, Fossett LK, Ramchandani P, Banner MP, Wein AJ, Seigalman ES, *et al*. Incidence of benign pathologic findings at partial nephrectomy for solitary renal mass presumed to be renal cell carcinoma on preoperative imaging. Urology 2006;68:737-40.
9. Saremi F, Knoll AN, Bendavid OJ, Schultze-Haakh H, Narula N, Sarlati F. Characterization of genitourinary lesions with diffusion-weighted imaging. Radiographics 2009;29:1295-317.
10. Squillaci E, Manenti G, Di Stefano F, Miano R, Strigari L, Simonetti G. Diffusion-weighted MR imaging in the evaluation of renal tumours. J Exp Clin Cancer Res 2004;23:39-45.
11. Cova M, Squillaci E, Stacul F, Manenti G, Gava S, Simonetti G, *et al*. Diffusion-weighted MRI in the evaluation of renal lesions: Preliminary results. Br J Radiol 2004;77:851-7.
12. Yoshikawa T, Kawamitsu H, Mitchell DG, Ohno Y, Ku Y, Seo Y, *et al*. ADC measurement of abdominal organs and lesions using parallel imaging technique. AJR Am J Roentgenol 2006;187:1521-30.
13. Zhang J, Tehrani YM, Wang L, Ishill NM, Schwartz LH, Hricak H. Renal masses: Characterization with diffusion-weighted MR imaging-a preliminary experience. Radiology 2008;247:458-64
14. Taouli B, Thakur RK, Mannelli L, Kim S, Lee VS, Israel GM, *et al*. Renal lesions: Characterization with diffusion-weighted imaging versus contrast-enhanced MR imaging. Radiology 2009;251:398-407.
15. Kilickesmez O, Inci E, Atilla S, Tasdelen N, Yetimoglu B, Gurmen N, *et al*. Diffusion-weighted imaging of the renal and adrenal lesions. J Comput Assist Tomogr 2009;33:828-33.
16. Sandrasegaran K, Sundaram CP, Ramaswamy R, Akisik FM, Lin C, Aisen AM, *et al*. Usefulness of diffusion-weighted imaging in the evaluation of renal masses. AJR Am J Roentgenol 2010;194:438-45.
17. Goyal A, Sharma R, Bhalla AS, Gamanagatti S, Seth A, Iyer VK, *et al*. Diffusion-weighted MRI in renal cell carcinoma: A surrogate marker for predicting nuclear grade and histological subtype. Acta Radiol 2012;53:349-58.
18. Goyal A, Sharma R, Bhalla AS, Gamanagatti S, Seth A. Diffusion-weighted MRI in inflammatory renal lesions: All that glitters is not RCC! Eur Radiol 2013;23:272-9.
19. Goyal A, Sharma R, Bhalla AS, Gamanagatti S, Seth A. Pseudotumours in chronic kidney disease: Can diffusion-weighted MRI rule out malignancy. Eur J Radiol 2013;82:1870-6.
20. Namimoto T, Yamashita Y, Mitsuzaki K, Nakayama Y, Tang Y, Takahashi M. Measurement of the apparent diffusion coefficient in diffuse renal disease by diffusion-weighted echo-planar MR imaging. J Magn Reson Imaging JMRI 1999;9:832-7.
21. Thoeny HC, De Keyzer F, Oyen RH, Peeters RR. Diffusion-weighted MR imaging of kidneys in healthy volunteers and patients with parenchymal diseases: Initial experience. Radiology 2005;235:911-7.
22. Xu X, Fang W, Ling H, Chai W, Chen K. Diffusion-weighted MR imaging of kidneys in patients with chronic kidney disease: Initial study. Eur Radiol 2010;20:978-83.
23. Goyal A, Sharma R, Bhalla AS, Gamanagatti S, Seth A. Diffusion-weighted MRI in assessment of renal dysfunction. Indian J Radiol Imaging 2012;22:155-9.
24. Verswijvel G, Vandecaveye V, Gelin G, Griten M, Oyen R, Palmers Y, *et al*. Diffusion-weighted MR imaging in the evaluation of renal infection: Preliminary results. JBR-BTR 2002;85:100-3.
25. Goyal A, Gadodia A, Sharma R. Xanthogranulomatous pyelonephritis: An uncommon pediatric renal mass. Pediatr Radiol 2010;40:1962-3.
26. Kang SK, Chandarana H. Contemporary imaging of the renal mass. Urol Clin North Am 2012;39:161-70.
27. Schatz SM, Lieber MM. Update on oncocytoma. Curr Urol Rep 2003;4:30-5.
28. Li G, Cuilleron M, Gentil-Perret A, Tostain J. Characteristics of image-detected solid renal masses: Implication for optimal treatment. Int J Urol 2004;11:63-7.
29. Israel GM, Bosniak MA. Pitfalls in renal mass evaluation and how to avoid them. Radiographics 2008;28:1325-38.
30. Pedrosa I, Sun MR, Spencer M, Olumi AF, Dewolf WC, Rofsky NM, *et al*. MR imaging of renal masses: Correlation with findings at surgery and pathologic analysis. Radiographics 2008;28:985-1003.
31. Young JR, Margolis D, Sauk S, Pantuck AJ, Sayre J, Raman SS. Clear cell renal cell carcinoma: Discrimination from other renal cell carcinoma subtypes and oncocytoma at multiphasic multidetector CT. Radiology 2013;267:444-53.
32. Kim JI, Cho JY, Moon KC, Lee HJ, Kim SH. Segmental enhancement inversion at biphasic multidetector CT: Characteristic finding of small renal oncocytoma. Radiology 2009;252:441-8.
33. Sasiwimonphan K, Takahashi N, Leibovich BC, Carter RE, Atwell TD, Kawashima A. Small (<4 cm) renal mass: Differentiation of angiomyolipoma without visible fat from renal cell carcinoma utilizing MR imaging. Radiology 2012;263:160-8.
34. Tanaka H, Yoshida S, Fujii Y, Tanaka H, Koga F, Saito K, *et al*. Diffusion-weighted magnetic resonance imaging in the differentiation of angiomyolipoma with minimal fat from clear cell renal cell carcinoma. Int J Urol 2011;18:727-30.
35. Catalano C, Fraioli F, Laghi A, Napoli A, Pediconi F, Nardis P, *et al*. High-resolution multidetector CT in the preoperative evaluation

of patients with renal cell carcinoma. AJR Am J Roentgenol 2003;180:1271-7.

36. Catalano OA, Choy G, Zhu A, Hahn PF, Sahani DV. Differentiation of malignant thrombus from bland thrombus of the portal vein in patients with hepatocellular carcinoma: Application of diffusion-weighted mr imaging. Radiology 2010;254:154-62.
37. Hallscheidt P, Pomer S, Roeren T, Kauffmann GW, Staehler G. Preoperative staging of renal cell carcinoma with caval thrombus: Is staging in MRI justified? Prospective histopathological correlated study. Urologe A 2000;39:36-40.